

# Aromaticity and electronic delocalization in all-metal clusters with single, double, and triple aromatic character

Ferran Feixas · Eduard Matito · Miquel Duran ·  
Jordi Poater · Miquel Solà

Received: 4 July 2010/Accepted: 23 August 2010/Published online: 16 September 2010  
© Springer-Verlag 2010

**Abstract** A series of monocyclic planar inorganic compounds with single, double, and triple (anti)aromatic character has been studied. The electron delocalization and aromaticity of these compounds have been assessed by means of two-center and multicenter electronic delocalization indices and their  $\sigma$ -,  $\pi$ -, and  $\delta$ -components. Results show that these indices are excellent predictors of the  $\sigma$ -,  $\pi$ -, and  $\delta$ -aromatic character of all-metal and semimetal clusters.

**Keywords** Electronic multicenter delocalization indices · Inorganic rings · Aromaticity · DFT calculations

## 1 Introduction

There is hardly a need to stress the important role played by the concept of aromaticity in chemistry. Since the discovery in 1825 of benzene by Michael Faraday [1] and after almost two centuries of intense developments, aromaticity

remains a major research motivation in chemistry. In fact, the last decade has witnessed exciting advances in aromaticity. Among them, we can refer to the introduction of electronic indices [2, 3] as reliable measures of local aromaticity and the definition of more refined magnetic-based indicators [4], although undoubtedly the most important recent breakthrough in the field of aromaticity took place in 2001 when Boldyrev, Wang et al., observed for the first time aromaticity in  $\text{Al}_4^{2-}$ , an all-metal compound [5]. The rapid synthesis and characterization of new all-metal and semimetal clusters exhibiting aromaticity further fueled the interest in these systems [6–8]. At variance with the classical aromatic organic molecules that possess only  $\pi$ -electron delocalization, these clusters can have  $\sigma$ -,  $\pi$ -, and  $\delta$ - (involving d orbitals) [9–11] or even  $\phi$ - (involving f orbitals) [12] electron delocalization, exhibiting characteristics of what has been called multifold aromaticity [6–8, 13–16].

The presence of multifold aromaticity and the lack of all-metal and semimetal aromatic clusters that can serve as inorganic reference systems (like benzene does in classical aromatic organic molecules) make the measure of aromaticity in these new systems much more complicated. Indeed, most of the current available methods to quantify aromaticity have been designed to measure the aromaticity of organic molecules and take benzene or other aromatic organic molecules as a reference in their definitions. This is the case of, for instance, the structural-based harmonic oscillator model of aromaticity (HOMA) [17, 18] or the electronic-based descriptors such as the aromatic fluctuation (FLU) index [19], the bond order index of aromaticity (BOIA) [20], or the aromaticity descriptor  $\theta$  proposed by Matta and Hernández-Trujillo [21, 22]. Likewise, energetic-based indicators such as resonance energies (RE) or aromatic stabilization energies (ASE) [23] are difficult to

---

Published as part of the special issue celebrating theoretical and computational chemistry in Spain.

**Electronic supplementary material** The online version of this article (doi:10.1007/s00214-010-0805-8) contains supplementary material, which is available to authorized users.

---

F. Feixas · M. Duran · J. Poater · M. Solà (✉)  
Institut de Química Computacional and Departament de  
Química, Universitat de Girona, Campus de Montilivi,  
17071 Girona, Catalonia, Spain  
e-mail: miquel.sola@udg.edu

E. Matito  
Institute of Physics, University of Szczecin,  
70-451 Szczecin, Poland

compute accurately in all-metal clusters because of the lack of appropriate reference systems [13, 24]. Although indices relying on reference systems are not adequate for the study of chemical reactivity [25], these methods are quite popular in the organic aromaticity realm. However, they cannot be applied directly to inorganic clusters without further refinements. For the moment, the most widely used methods to discuss aromaticity in inorganic clusters are the basic electron counting based on the  $4n + 2$  Hückel's rule [26–29] and the magnetic-based indicators of aromaticity, in particular, the nucleus-independent chemical shifts (NICS) [30]. A great advantage of NICS, apart from being very accessible and easy to compute, is that it does not use reference values, so it can be easily applied to any molecule.

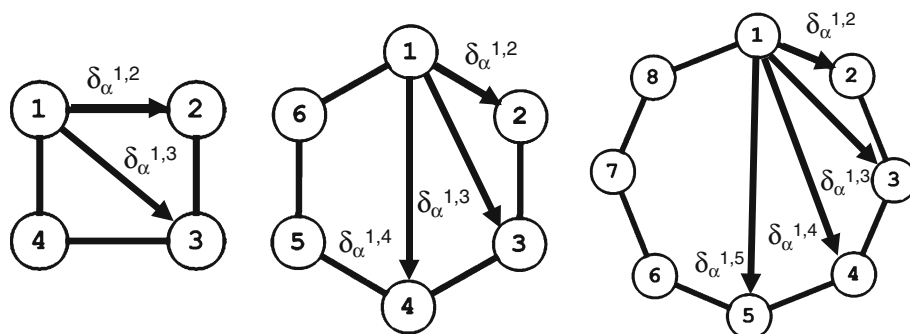
Less common is the use of electronic multicenter indices (MCI) [20, 31–34] to study multifold aromaticity in inorganic species [35–37]. As for NICS, the MCI definition is general and free from reference values. In recent work [38, 39], we have shown that MCI does an excellent work in inorganic aromatic clusters providing aromaticity trends that are superior to those furnished by NICS. An interesting property of the MCI index is that for planar systems with only  $\sigma$ - and  $\pi$ -occupied orbitals the total MCI value can be exactly decomposed into their  $\sigma$ - and  $\pi$ -components. For planar species with additional occupied orbitals of  $\delta$ -type, the separation into the different components is not exact because of some  $\sigma$ - and  $\delta$ -orbital mixing within a given atomic domain. However, the errors introduced by assuming exact separability in these systems turn out to be in general negligible (vide infra). The first aim of the present manuscript is to examine whether the separation of the MCI values into the  $\sigma$ -,  $\pi$ -, and  $\delta$ -components for a series of well-studied all-metal (anti)aromatic clusters can provide valuable information about the different  $\sigma$ -,  $\pi$ -, and  $\delta$ -contributions to the total aromatic character of the molecules.

We have also recently shown that changes in the so-called crossed contributions (for instance, the ortho-, meta-, and para-components in six-membered rings, 6-MRs) to the total  $\pi$ -electronic delocalization ( $\delta_\pi$ ) when two

electrons are added or removed for a given species can be used to distinguish between aromatic and antiaromatic systems [40, 41]. Thus, we have found that for benzene, ortho ( $\delta_\pi^{1,2}$ ) and para ( $\delta_\pi^{1,4}$ ) contributions increase and meta ( $\delta_\pi^{1,3}$ ) decreases from antiaromatic  $C_6H_6^{2+}$  or  $C_6H_6^{2-}$  to aromatic  $C_6H_6$ . Likewise, for the antiaromatic cyclobutadiene, from aromatic  $C_4H_4^{2+}$  to antiaromatic  $C_4H_4$  the  $\delta_\pi^{1,2}$  contribution increases and  $\delta_\pi^{1,3}$  decreases. Moreover, we found that the crossed term corresponding to the two farthest atoms in the ring (i.e.,  $\delta_\pi^{1,3}$  in 4-MRs,  $\delta_\pi^{1,4}$  in 6-MRs or  $\delta_\pi^{1,5}$  in 8-MRs, see Fig. 1) decreases in aromatic species when two electrons are added or removed, whereas the opposite is true for antiaromatic species [41]. It was reported that this crossed term is higher for the most aromatic molecule in a series of same-membered rings [41]. As a second main objective of this work, we want to investigate whether such alternation patterns are also present in the all-metal inorganic cluster  $Al_4^{2-}$ , not only for total  $\pi$ -electronic delocalization but also for the total  $\sigma$ -component of the electronic delocalization. In addition, we aim to know whether the crossed term corresponding to the two farthest atoms in the ring can be a good descriptor of aromaticity in all-metal and semimetal clusters.

To reach these goals, we have chosen a series of all-metal clusters with well-established aromatic character. In particular, we will discuss electron delocalization and aromaticity in some 4-MRs having, first, double  $\sigma$ - and  $\pi$ -aromaticity ( $Al_4^{2-}$  [5, 13, 24, 35, 36, 42–51],  $MAI_4^-$  ( $M = Li, Na, Cu$ ) [35, 49, 52, 53],  $Al_3Ge^-$  [54],  $Al_2Ge_2$  [16, 55],  $AlGe_3^+$  [56], and  $Ge_4^{2+}$  [56]), and, second,  $\sigma$ -aromaticity and  $\pi$ -antiaromaticity (the  $Al_4^{4-}$  unit attached to  $Li^+$  cations,  $Li_xAl_4^{\pm}$ ) [49–51, 57, 58]. Then, we have selected a series of transition-metal 3-MRs with single  $\sigma$ -aromaticity ( $Cu_3^+$ ) [59], conflicting  $\sigma$ -aromaticity ( $Cu_3H_3$ ) [60], double  $\sigma$ - and  $\pi$ -aromaticity ( $Y_3^-$  and  $La_3^-$ ) [61], double  $\pi$ - and  $\delta$ -aromaticity ( $Ta_3O_3^-$ ) [10], and finally, triple  $\sigma$ -,  $\pi$ -, and  $\delta$ -aromaticity ( $Hf_3$ ) [11, 62]. In addition, the aromaticity of two open-shell species,  $^5Ta_3^-$  [62] and  $^3Hf_3$  [11], will be analyzed in detail. We shall reach the conclusion, which we anticipate here, that both MCI and the analysis of crossed contributions to the total

**Fig. 1** Decomposition of electron delocalization in crossed-terms  $\delta_\alpha^{1,x}$  ( $\alpha = \sigma, \pi, \delta, \dots$ ) for four-, six-, and eight-membered rings



$\sigma$ -,  $\pi$ -, and  $\delta$ -electronic delocalization are excellent indicators of  $\sigma$ -,  $\pi$ -, and  $\delta$ -aromaticity in inorganic clusters.

## 2 Computational details

All calculations reported in this work were performed by means of the Gaussian03 [63] computational package. The gas-phase optimized geometries reported here were calculated in the framework of density-functional theory (DFT) using the B3LYP functional [64] which combines the three-parameter Becke's exchange non-local functional [65] and the Lee–Yang–Parr's correlation non-local functional [66]. The 6–311+G(d) basis set [67, 68] was used for all calculations, except for the study of the  $\text{Cu}_3^+$ ,  $\text{Cu}_3\text{H}_3$ ,  $\text{Y}_3^-$ ,  $\text{La}_3^-$ ,  $\text{Ta}_3\text{O}_3^-$ ,  $\text{Hf}_3$ ,  ${}^5\text{Ta}_3^-$ , and  ${}^3\text{Hf}_3$  species for which we have used the Stuttgart 14-valence-electron pseudopotentials and the valence basis sets augmented with two f-type polarization functions [69, 70] in order to take into account relativistic effects. In  $\text{Cu}_3\text{H}_3$  and  $\text{Ta}_3\text{O}_3^-$ , the aug-cc-pVTZ basis set [71, 72] was used for the H and O atoms. To ensure that a minimum on the potential energy surface (PES) was obtained, we carried out vibrational frequency calculations at the same level, either B3LYP/6–311+G(d) or B3LYP/X/Stuttgart+2f (X = Cu, Y, La, Ta, and Hf).

We report here results for an unstable dianion such as  $\text{Al}_4^{2-}$ . In a recent work, Lambrecht et al. [73] have shown that  $\text{Al}_4^{2-}$  is unstable when compared to  $\text{Al}_4^- + \text{free e}^-$  and, consequently, its properties change significantly when increasing the number of diffuse functions in the basis set. Indeed, after inclusion of certain number of diffuse functions, the  $\text{Al}_4^{2-}$  evolves to  $\text{Al}_4^- + \text{free e}^-$ . In this sense, Lambrecht et al. [73] warned about the validity of calculations carried out for such unstable dianions. In a recent comment [74] (see also the rebuttal in Ref. [75]) on the work by Lambrecht et al. [73], Zubarev and Boldyrev argued against this point of view and considered that the bound state of the individual  $\text{Al}_4^{2-}$  is an adequate model of  $\text{Al}_4^{2-}$  in a stabilizing environment such as in  $\text{LiAl}_4^-$  or  $\text{Li}_2\text{Al}_4$ . They also considered that calculations for isolated  $\text{Al}_4^{2-}$  species using a 6–311+G(d) basis provide an accurate model for the  $\text{Al}_4^{2-}$  unit embedded in a stabilizing environment. Following the Zubarev and Boldyrev arguments [74], we will discuss the properties of the bound state of  $\text{Al}_4^{2-}$  by employing the 6–311+G(d) basis set. The same hypothesis has been assumed in the calculations of the isolated  $\text{Al}_4^{4-}$  and  $\text{Li}_2\text{Al}_4^{2-}$  species.

In this work, we measure the electron delocalization by means of the so-called delocalization indices (DIs), or in a more general nomenclature, the electron sharing indices (ESIs) [76–78]. The ESI value between atoms A and B,  $\delta(A,B)$  is obtained by double integration of the exchange-

correlation density ( $\gamma_{XC}(\vec{r}_1, \vec{r}_2)$ ) [79] over the molecular space regions corresponding to atoms A and B,

$$\delta(A,B) = -2 \int_A \int_B \gamma_{XC}(\vec{r}_1, \vec{r}_2) d\vec{r}_1 d\vec{r}_2 \quad (1)$$

For monodeterminantal wave functions, one obtains:

$$\delta(A,B) = 2 \sum_{i,j}^{\text{occ.MSO}} S_{ij}(A)S_{ij}(B) \quad (2)$$

The summations in Eq. (2) run over all occupied molecular spin-orbitals (MSOs).  $S_{ij}(A)$  is the overlap between MOs  $i$  and  $j$  within the molecular space assigned to atom A.  $\delta(A,B)$  provides a quantitative idea of the number of electrons delocalized or shared between atoms A and B.

To study the delocalization effects upon extraction or addition of two electrons, we calculate the total delocalization, which for planar systems with only  $\sigma$ - and  $\pi$ -occupied orbitals can be exactly split ( $S_{\sigma\pi}(A) = 0$ ) into the  $\sigma$ - and  $\pi$ -contributions.

$$\begin{aligned} \delta_{\text{tot}} &= \sum_{A_i, A_j \neq A_j} \delta(A_i, A_j) = \sum_{A_i, A_j \neq A_j} \delta_\pi(A_i, A_j) \\ &+ \sum_{A_i, A_i \neq A_j} \delta_\sigma(A_i, A_j) = \delta_\pi + \delta_\sigma \end{aligned} \quad (3)$$

In the case of species with occupied orbitals of  $\delta$ -symmetry, we have also computed the  $\delta_\delta$  component (see Supporting Information), although in this case the separation in  $\delta_\sigma$ ,  $\delta_\pi$ , and  $\delta_\delta$  is not strictly exact.

In addition,  $\delta_\alpha$  ( $\alpha = \sigma, \pi$ , and  $\delta$ ) can be split into the different crossed contributions in the ring. For instance, for a given four-membered ring (4-MR) we have ortho- (1,2) and meta- (1,3) terms (see Fig. 1). In our study, we have considered averaged values for the crossed terms, so in a 4-MR we have:

$$\begin{aligned} \delta_\alpha &= 4\delta_\alpha^{1,2} + 2\delta_\alpha^{1,3} \\ \delta_\alpha^{1,2} &= \frac{\delta_\alpha(1,2) + \delta_\alpha(2,3) + \delta_\alpha(3,4) + \delta_\alpha(1,4)}{4} \\ \delta_\alpha^{1,3} &= \frac{\delta_\alpha(1,3) + \delta_\alpha(2,4)}{2} \end{aligned} \quad (4)$$

For the aromaticity analysis, we have also applied the multicenter index (MCI) [20, 32]. MCI is a particular extension of the  $I_{\text{ring}}$  index [31].

$$I_{\text{ring}}(\mathcal{A}) = \sum_{i_1, i_2, \dots, i_N} n_{i_1} \dots n_{i_N} S_{i_1 i_2}(A_1) S_{i_2 i_3}(A_2) \dots S_{i_N i_1}(A_N) \quad (5)$$

$n_i$  being the occupancy of MO  $i$  and  $\mathcal{A} = \{A_1, A_2, \dots, A_N\}$  a string containing the set of  $N$  atoms forming the ring structure. Summing up all  $I_{\text{ring}}$  values resulting from the

permutations of indices  $A_1, A_2, \dots, A_N$ , the mentioned MCI index [32] is defined as:

$$\text{MCI}(\mathcal{A}) = \frac{1}{2N} \sum_{P(\mathcal{A})} I_{\text{ring}}(\mathcal{A}) \quad (6)$$

where  $P(\mathcal{A})$  stands for a permutation operator that interchanges the atomic labels  $A_1, A_2, \dots, A_N$  to generate the  $N!$  permutations of the elements in the string  $\mathcal{A}$  [20, 34]. MCI and  $I_{\text{ring}}$  give an idea of the electron sharing between all atoms in the ring. The more positive the MCI values [32, 33, 80], the more aromatic the rings. For planar species with only  $\sigma$ - and  $\pi$ -occupied orbitals, the MCIs like the DIs can be exactly split into the  $\sigma$ - and  $\pi$ -contributions:

$$\text{MCI}(\mathcal{A}) = \text{MCI}_\sigma(\mathcal{A}) + \text{MCI}_\pi(\mathcal{A}) \quad (7)$$

In planar systems with  $\sigma$ - and  $\delta$ -occupied orbitals, the exact separation between the  $\sigma$ - and  $\delta$ -components is not possible. In addition, in non-planar systems MCI cannot be exactly separated into  $\sigma$ -,  $\pi$ -, and  $\delta$ -components. In these cases, we have partitioned MCI into the different contributions in two different ways. First through Eqs. (8–10) by adding the orbital contributions of those orbitals that belong to (or are assumed to belong to) a given symmetry  $\alpha$  ( $\alpha = \sigma, \pi$ , and  $\delta$ ):

$$\text{MCI}(\mathcal{A}) = \sum_{\alpha=\sigma,\pi,\delta,\dots} \text{MCI}_\alpha^{\text{orb}}(\mathcal{A}) \quad (8)$$

$$\text{MCI}_\alpha^{\text{orb}}(\mathcal{A}) = \frac{1}{2N} \sum_{P(\mathcal{A})} I_{\text{ring},\alpha}^{\text{orb}}(\mathcal{A}) \quad (9)$$

$$I_{\text{ring},\alpha}^{\text{orb}}(\mathcal{A}) = \sum_{i_1 \in \alpha, i_2, \dots, i_N} n_{i_1} \dots n_{i_N} S_{i_1 i_2}(A_1) S_{i_2 i_3}(A_2) \dots S_{i_N i_1}(A_N) \quad (10)$$

In this way, the sum of all  $\text{MCI}_\alpha^{\text{orb}}$  yields the exact MCI, but in each  $\text{MCI}_\alpha^{\text{orb}}$  some mixing from MOs of different symmetry than  $\alpha$  is possible. This was the method used in a previous work to separate DIs into their molecular orbital contributions [81]. An alternative is to substitute Eq. (10) by (11) that assumes  $S_{\alpha\beta}(A) = 0$  ( $\alpha, \beta = \sigma, \pi$ , and  $\delta$ ) for  $\alpha \neq \beta$ :

$$I_{\text{ring},\alpha}^{\text{ovl}}(\mathcal{A}) = \sum_{i_1 \in \alpha, i_2 \in \alpha, \dots, i_N \in \alpha} n_{i_1} \dots n_{i_N} S_{i_1 i_2}(A_1) S_{i_2 i_3}(A_2) \dots S_{i_N i_1}(A_N) \quad (11)$$

Then, we have:

$$\text{MCI}_\alpha^{\text{ovl}}(\mathcal{A}) = \frac{1}{2N} \sum_{P(\mathcal{A})} I_{\text{ring},\alpha}^{\text{ovl}}(\mathcal{A}) \quad (12)$$

and

$$\text{MCI}(\mathcal{A}) \approx \text{MCI}^{\text{ovl}}(\mathcal{A}) = \sum_{\alpha=\sigma,\pi,\delta,\dots} \text{MCI}_\alpha^{\text{ovl}}(\mathcal{A}) \quad (13)$$

MCI is equal to  $\text{MCI}^{\text{ovl}}$  when the partition between the different components is exact. Otherwise MCI and  $\text{MCI}^{\text{ovl}}$  can differ, and the difference is a measure of the error made in the separation.  $\text{MCI}^{\text{ovl}}$  could be higher or lower than the exact MCI depending on the positive or negative contributions of the overlap products containing  $S_{\alpha\beta}(A)$  terms. Despite not being strictly separable (vide supra), for systems with  $\delta$ -orbitals we report MCIs values split into  $\sigma$ -,  $\pi$ -, and  $\delta$ -components in the same way that we have described above. This feature is especially interesting to evaluate multifold aromaticity in all-metal clusters.

Finally, although several atomic partitions may be used for the calculations of the overlap between MOs  $i$  and  $j$  within the molecular space assigned to atom  $A$  [35, 78, 82, 83] to obtain both the DIs and MCIs, we have chosen in the present work the partition carried out in the framework of the quantum theory of atoms-in-molecules (QTAIM) of Bader [84–86], by which atoms are defined from the condition of zero-flux gradient in the one-electron density,  $\rho(\mathbf{r})$ . Calculation of overlap matrices and computation of MCI have been performed with the AIMPAC [87] and ESI-3D [88] collection of programs.<sup>1</sup> For molecules containing Ta and Hf, the QTAIM partition failed due to the presence of non-nuclear attractors, regions that cannot be directly associated with a given atomic region. In these cases, we used the “fuzzy atom” partition [89, 90] in which the atomic domains do not have boundaries. Instead, at every point  $\mathbf{r}$  of the space a weight factor  $w_A(\mathbf{r})$  is defined for each atom,  $A$ , to measure to which extent the given point belongs to atom  $A$ . These atomic weight factors are chosen to be non-negative and satisfy the following condition when summing over all atoms of the system:

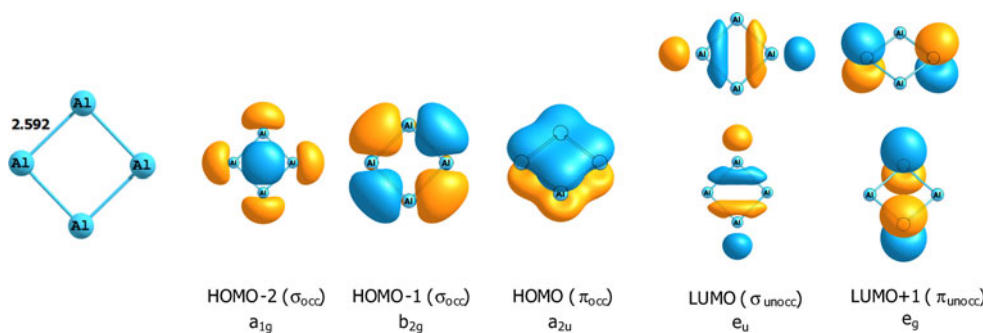
$$\sum_A w_A(\mathbf{r}) = 1 \quad (14)$$

where overlap matrix elements for an atom  $A$  are now:

$$S_{ij}(A) = \int \varphi_i^*(\mathbf{r}) w_A(\mathbf{r}) \varphi_j(\mathbf{r}) d\mathbf{r} \quad (15)$$

<sup>1</sup> The numerical accuracy of the QTAIM calculations has been assessed using two criteria: (1) The integration of the Laplacian of the electron density ( $\nabla^2 \rho(\mathbf{r})$ ) within an atomic basin must be close to zero; and (2) The number of electrons in a molecule must be equal to the sum of all the electron populations of the molecule. For all atomic calculations, integrated absolute values of  $\nabla^2 \rho(\mathbf{r})$  were always less than 0.001 a.u.. For all molecules, errors in the calculated number of electrons were always below 0.01 a.u.. It is important to mention that the default maximum distance from the nucleus used to integrate the atomic region has to be increased when diffuse functions are employed in the presence of metal atoms. In the AIMPAC program, the default integration maximum distance is 9.0 a.u.. However, we have found that this distance should be increased to 12.0 a.u. for the proper integration of Al and Ge atoms. If this value is not increased, the sum of all electron populations will not be equal to the number of electrons in a molecule. Consequently, these integration distances have to be changed in the input file.

**Fig. 2** The low-lying occupied and unoccupied molecular orbitals of  $\text{Al}_4^{2-}$



“Fuzzy atom” DIs and MCIs were calculated with the FUZZY code [89, 91], which implements a Becke’s multi-center integration algorithm with Chebyshev and Lebedev radial and angular quadratures, respectively. A grid of 60 radial by 900 angular points per atom has been used in all cases. We have employed the Becke’s algebraic function with the recommended stiffness parameter  $k = 3$ . We have used the set of atomic radii determined by Koga [92].

### 3 Results and discussion

In this section, we first discuss the  $\text{Al}_4^{2-}$  compound and related species, in particular the  $[\text{Al}_n\text{Ge}_{4-n}]^{q\pm}$  ( $n = 0\text{--}4$ ) series, in detail. Then, the multifold aromaticity of  $\text{Cu}_3^+$ ,  $\text{Cu}_3\text{H}_3$ ,  $\text{Y}_3^-$ ,  $\text{La}_3^-$ ,  $\text{Ta}_3\text{O}_3^-$ ,  $\text{Hf}_3$ ,  ${}^5\text{Ta}_3^-$ , and  ${}^3\text{Hf}_3$  compounds is analyzed.

$\text{Al}_4^{2-}$  is the quintessential all-metal aromatic cluster. The B3LYP/6-311+G(d) molecular structure and the lowest-lying occupied and unoccupied orbitals of  $\text{Al}_4^{2-}$  are depicted in Fig. 2.  $\text{Al}_4^{2-}$  contains a pair of delocalized  $\pi$ -electrons and two pairs of  $\sigma$ -electrons that contribute to the overall aromaticity of this species [5, 43, 47]. The two  $\pi$ -electrons obey the  $4n + 2$  Hückel rule for monocyclic  $\pi$ -systems [26–29]. Although this is not the case for the  $\sigma$  electrons, it was found that the two pairs of delocalized  $\sigma$  electrons belong to molecular orbitals that follow orthogonal radial and tangential directions, which makes them to be totally independent [48], thus separately following the  $4n + 2$  rule. The aromaticity of  $\text{Al}_4^{2-}$  has been confirmed by four criteria of aromaticity: energetic (resonance energies [13, 24, 48]), structural (planarity with equal bond lengths [5]), magnetic (ring currents [47, 49]), induced magnetic field analysis [51], and nucleus-independent chemical shifts (NICS) values [6, 36] and electronic (electron localization function (ELF) [93]) plots [45], hardness and polarizability values [46], and MCI results [35, 36, 38].

Table 1 lists the MCI and  $\delta^{1,3}$  values and their  $\sigma$ - and  $\pi$ -components for  $\text{Al}_4$ ,  $\text{Al}_4^{2-}$ , and  $\text{Al}_4^{4-}$  species. The MCI and  $\text{MCI}_\pi$  values obtained for  $\text{Al}_4^{2-}$  are 0.356 and

**Table 1** MCI,  $\text{MCI}_\alpha$ ,  $\delta^{1,3}$ , and  $\delta_\alpha^{1,3}$  ( $\alpha = \sigma$  and  $\pi$ ) indices for the  $\text{Al}_4$ ,  $\text{Al}_4^{2-}$ , and  $\text{Al}_4^{4-}$  units at the B3LYP/6-311+G(d) level of theory

	$\text{N} - 2_{(2\pi \text{ e}-)}$ $\text{Al}_4$ ( $a_{1g}$ ) <sup>a</sup>	$\text{N} - 2_{(0\pi \text{ e}-)}$ $\text{Al}_4$ ( $a_{2u}$ ) <sup>a</sup>	$\text{N} - 2_{(2\pi \text{ e}-)}$ $\text{Al}_4$ ( $b_{2g}$ ) <sup>a</sup>	$\text{N}_{(2\pi \text{ e}-)}$ $\text{Al}_4^{2-}$	$\text{N} + 2_{(4\pi \text{ e}-)}$ $\text{Al}_4^{4-}$ ( $e_g$ ) <sup>b</sup>
MCI	0.197	0.182	0.325	0.356	0.222
$\text{MCI}_\sigma$	0.010	0.182	0.138	0.169	0.210
$\text{MCI}_\pi$	0.187	0.000	0.187	0.187	0.012
$\delta^{1,3}$	0.437	0.551	0.710	0.817	0.629
$\delta_\sigma^{1,3}$	0.187	0.551	0.460	0.567	0.540
$\delta_\pi^{1,3}$	0.250	0.000	0.250	0.250	0.089
Aromaticity	$\pi$	$\sigma$	$\sigma + \pi$	$\sigma + \pi$	$\sigma$

All values in atomic units

<sup>a</sup> Orbital from which two electrons have been removed (see Fig. 1)

<sup>b</sup> Orbital to which two electrons have been added (see Fig. 1)

0.187 a.u., respectively. The value of the  $\text{MCI}_\pi$  (0.1875 a.u. for a monodeterminantal wave function) can be easily obtained from symmetry arguments for any ring  $X_4$  of  $D_{4h}$  symmetry with only  $2\pi$ -electrons occupying the same orbital such as in  $\text{Al}_4^{2-}$  [38]. Our results indicate that the  $\pi$  delocalization in the  $\text{Al}_4^{2-}$  species is slightly larger than the  $\sigma$  one (0.187 vs. 0.169 a.u.). This is in line with the previous dissected NICS results [35, 38], showing that  $\text{NICS}(0)_\pi$  is somewhat more negative than  $\text{NICS}(0)_\sigma$  and also with the result from the ELF indicating higher  $\pi$ - than  $\sigma$ -aromaticity in  $\text{Al}_4^{2-}$  [45], but in contrast with the fact that the ring current in  $\text{Al}_4^{2-}$  has a negligible contribution from the two  $\pi$ -electron system [43, 44]. According to the  $\text{MCI}_\sigma$  and  $\text{MCI}_\pi$  values  $\text{Al}_4^{2-}$  is  $\sigma$ - and  $\pi$ -aromatic. Adding two electrons to one of the two LUMO+1 orbitals of  $\text{Al}_4^{2-}$  of  $e_g$  symmetry, we reach the singlet  $\text{Al}_4^{4-}$  species with four  $\pi$ -electrons. The singlet  $\text{Al}_4^{4-}$  species in this particular electronic state (two electrons in an  $e_g$  orbital) is not a true minimum. This is the only species among those reported in this work that it is not a minimum. In spite of that we discuss it here because the analysis of electron delocalization in this system gives interesting insight. As it can be seen in the values of Table 1, addition of these two electrons leads to an antiaromatic  $4\pi$ -electron system as reflected by the important reduction in the  $\text{MCI}_\pi$  value when going from  $\text{Al}_4^{2-}$  to  $\text{Al}_4^{4-}$ . There is also some increase in the  $\text{MCI}_\sigma$  indicating that the  $\text{Al}_4^{4-}$  unit has

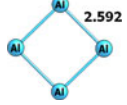
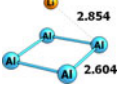
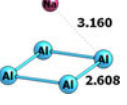
preserved the  $\sigma$ -aromatic character. Removal of two electrons from the  $\text{Al}_4^{2-}$  species can be performed from different orbitals leading to different states of the  $\text{Al}_4$  unit. If one removes two electrons from the  $b_{2g}$  orbital, the effect on the MCI values is minor with a slight reduction in the  $\text{MCI}_{\sigma}$  value. On the other hand, if one takes out two electrons from the  $a_{1g}$  orbital of  $\text{Al}_4^{2-}$ , the reduction in the  $\text{MCI}_{\sigma}$  value is huge leading to an  $\text{Al}_4$  unit with only  $\pi$ -aromaticity. This result is in agreement with the fact that according to the decomposition of the NICS into their canonical molecular orbital (CMO) components [94], the tangential  $b_{2g}$  orbital has a paratropic contribution to NICS ( $\text{NICS}(b_{2g}) = +10.8$  ppm), while the radial  $a_{1g}$  orbital sustains a diatropic current ( $\text{NICS}(a_{1g}) = -3.9$  ppm). Therefore, both the MCI and NICS point out that the contribution to the  $\sigma$ -aromaticity in  $\text{Al}_4^{2-}$  species of the two electrons in the radial  $\sigma$ -orbital is more important than that from the two electrons in the tangential  $\sigma$ -orbital. Finally, removal of the two electrons from the  $a_{2u}$  orbital of  $\pi$ -symmetry results in a system with a significant  $\text{MCI}_{\sigma}$  value and  $\sigma$ -aromatic character.

MCI gives valuable information about the type of aromaticity ( $\sigma$ ,  $\pi$ , or  $\delta$ ) present in all-metal clusters. In addition, it correctly orders a series of clusters according to their aromaticity [41]. It has, however, the problem that it does not provide information about antiaromaticity since in both non- and antiaromatic species electrons are localized and the MCI value is close to zero for the two cases [34]. Discrimination between non- and antiaromatic species can be achieved by analyzing the crossed term corresponding

to the two farthest atoms in the ring (i.e.,  $\delta_{\alpha}^{1,3}$  in 4-MRs). This term decreases in aromatic species when two electrons are added or removed, whereas the opposite is true for antiaromatic species [41]. For non-aromatic species, this term suffers only minor changes upon addition or extraction of two electrons. Results in Table 1 confirm this trend for  $\text{Al}_4^{2-}$ . Thus, addition of two electrons to the  $e_g$  LUMO+1 orbital of  $\text{Al}_4^{2-}$  transforms a  $\sigma$ - and  $\pi$ -aromatic  $\text{Al}_4^{2-}$  into a  $\sigma$ -aromatic and  $\pi$ -antiaromatic  $\text{Al}_4^{4-}$  system and the  $\delta_{\alpha}^{1,3}$  decreases as expected, while the  $\delta_{\sigma}^{1,3}$  remains more or less the same. The same situation is found when the two electrons are removed from the  $a_{2u}$  orbital. On the other hand, if the electrons are removed from the  $a_{1g}$   $\sigma$ -orbital  $\delta_{\pi}^{1,3}$  does not change and  $\delta_{\sigma}^{1,3}$  decreases. A decrease is also seen for the withdrawal of two electrons from the tangential  $\sigma$   $b_{2g}$  orbital, although the reduction of the  $\delta_{\sigma}^{1,3}$  is minor in this case, again indicating that the radial contribution to the  $\sigma$ -aromaticity is larger than that of the tangential orbital. As for organic aromatic molecules [41], the change of  $\delta_{\alpha}^{1,3}$  ( $\alpha = \sigma$ ,  $\pi$ , and  $\delta$ ) in 4-MRs when adding or removing two electrons is a good indicator of  $\alpha$ -(anti)aromaticity. It has the additional advantage with respect to MCI of being a computationally much cheaper descriptor.

Tables 2 and 3 gather the values of MCI and  $\delta^{1,3}$  values and their  $\sigma$ - and  $\pi$ -contributions for  $\text{Al}_4^{2-}$  and  $\text{Al}_4^{4-}$  species coordinated to  $\text{Li}^+$ ,  $\text{Na}^+$ , and  $\text{Cu}^+$  cations to form pyramidal  $\text{C}_{4v}$  complexes, which are more stable than the planar  $\text{C}_{2v}$  isomers [53]. The MCI and  $\delta^{1,3}$  values of Table 2 indicate a reduction in aromaticity in the order

**Table 2** MCI,  $\text{MCI}_{\alpha}$ ,  $\delta^{1,3}$ , and  $\delta_{\alpha}^{1,3}$  ( $\alpha = \sigma$  and  $\pi$ ) indices for the  $\text{Al}_4$  unit in  $\text{Al}_4^2$ ,  $\text{LiAl}_4^-$ ,  $\text{NaAl}_4^-$ , and  $\text{CuAl}_4^-$  at the B3LYP/6-311+G(d) level of theory

	$\text{N}_{(2\pi \text{ e}-)}$ $\text{Al}_4^{2-}$	$\text{N}_{(2\pi \text{ e}-)}$ $\text{LiAl}_4^-$	$\text{N}_{(2\pi \text{ e}-)}$ $\text{NaAl}_4^-$	$\text{N}_{(2\pi \text{ e}-)}$ $\text{CuAl}_4^-$	
	2.592		2.854 2.604		3.160 2.608
MCI	0.356	0.288	0.234	0.129	
$\text{MCI}_{\sigma}^{\text{orb}}$	0.169	0.156	0.157	0.111	
$\text{MCI}_{\pi}^{\text{orb}}$	0.187	0.132	0.077	0.018	
$\text{MCI}^{\text{ovl}}$	0.356	0.287	0.234	0.106	
$\text{MCI}_{\sigma}^{\text{ovl}}$	0.169	0.153	0.157	0.084	
$\text{MCI}_{\pi}^{\text{ovl}}$	0.187	0.134	0.077	0.022	
Error (%) <sup>a</sup>	0	0.33	0	17.84	
$\delta^{1,3}$	0.817	0.761	0.708	0.539	
$\delta_{\sigma}^{1,3}$	0.567	0.547	0.549	0.450	
$\delta_{\pi}^{1,3}$	0.250	0.214	0.159	0.089	

All distances in Å and all delocalization values in atomic units

<sup>a</sup> Calculated as  $\left| \frac{\text{MCI} - \text{MCI}^{\text{ovl}}}{\text{MCI}} \right| \times 100$

**Table 3** MCI, MCI<sub>σ</sub>, δ<sup>1,3</sup>, and δ<sub>π</sub><sup>1,3</sup> ( $\alpha = \sigma$  and  $\pi$ ) indices for the Al<sub>4</sub> unit in Al<sub>4</sub><sup>2-</sup>, LiAl<sub>4</sub><sup>-</sup>, Li<sub>2</sub>Al<sub>4</sub><sup>-</sup>, Li<sub>3</sub>Al<sub>4</sub><sup>2-</sup>, and Li<sub>4</sub>Al<sub>4</sub> at the B3LYP/6-311+G(d) level of theory

	D <sub>4h</sub> (2π e-) Al <sub>4</sub> <sup>2-</sup>	N <sub>(2π e-)</sub> LiAl <sub>4</sub> <sup>-</sup>	N <sub>(2π e-)</sub> Li <sub>2</sub> Al <sub>4</sub> <sup>-</sup>	N <sub>(4π e-)</sub> Li <sub>3</sub> Al <sub>4</sub> <sup>2-</sup>	N <sub>(4π e-)</sub> Li <sub>4</sub> Al <sub>4</sub>
MCI	0.356	0.288	0.282	0.214	0.154
MCI <sub>σ</sub> <sup>orb</sup>	0.169	0.156	0.155	0.155	0.136
MCI <sub>π</sub> <sup>orb</sup>	0.187	0.132	0.127	0.059	0.018
MCI <sub>σ</sub> <sup>ovl</sup>	0.356	0.287	0.287	0.240	0.164
MCI <sub>π</sub> <sup>ovl</sup>	0.169	0.153	0.146	0.159	0.144
MCI <sub>σ</sub> <sup>ovl</sup>	0.187	0.134	0.141	0.081	0.020
Error (%) <sup>a</sup>	0	0.33	2.38	12.41	7.40
δ <sup>1,3</sup>	0.817	0.761	0.738	0.627	0.598
δ <sub>σ</sub> <sup>1,3</sup>	0.567	0.547	0.520	0.500	0.502
δ <sub>π</sub> <sup>1,3</sup>	0.250	0.214	0.218	0.128	0.089

All distances in Å and all delocalization values in atomic units

<sup>a</sup> Calculated as  $\left| \frac{MCI - MCI^{ref}}{MCI} \right| \times 100$

$\text{Al}_4^{2-} > \text{LiAl}_4^- > \text{NaAl}_4^- > \text{CuAl}_4^-$ . Similar MCI values were reported by Mandado et al. [35] and Roy et al. [36]. The reason for the differences found in the MCI of  $\text{Al}_4^{2-}$  reported by Mandado et al. [35] and ours has been discussed in a previous paper [38] (see also footnote 1). It is worth to mention that because of the loss of symmetry in some compounds, as  $\text{MAl}_4^-$  ( $\text{M} = \text{Li}^+$ ,  $\text{Na}^+$ , and  $\text{Cu}^+$ ) or the systems from Table 3, one should talk about pseudo- $\pi$  instead of  $\pi$  orbitals in these species. However, the overlap between  $\sigma$  and  $\pi$  occupied molecular orbitals is almost zero for Li and Na compounds. We have calculated the relative error between the MCI and  $\text{MCI}_{\text{ovl}}$  values and in both cases is lower than 1%. The only exception is the  $\text{CuAl}_4^-$  where the error is larger and close to 18% [35]. The reduction in the MCI and  $\delta^{1,3}$  values due to metal cation coordination is more important for the  $\pi$ - than for the  $\sigma$ -component, and it is due to the partial transfer of the  $2\pi$ -electrons from  $\text{Al}_4^{2-}$  to the cation. Indeed, the electronic charge of the  $\text{Al}_4$  unit obtained by Mandado et al. using QTAIM and Hirshfeld populations shows a decrease from  $\text{LiAl}_4^-$  to  $\text{CuAl}_4^-$  species [35]. This decrease in electronic delocalization when going from  $\text{Al}_4^{2-}$  to  $\text{MAl}_4^-$  ( $\text{M} = \text{Li}$ ,  $\text{Na}$ , or  $\text{Cu}$ ) is similar to that found in  $\text{Mg}_3^{2-}$  when coordinated to alkali-metals cations [37]. The reduction in aromaticity of  $\text{Al}_4^{2-}$  due to  $\text{Li}^+$  and  $\text{Cu}^+$   $\text{C}_{4v}$  coordination was also indicated by Sundholm et al. [42] from the calculation of nuclear magnetic shieldings and by Roy et al. [36] from NICS values.

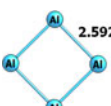
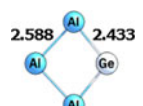
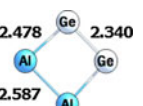
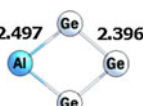
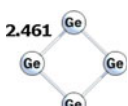
The results of Table 3 show that going from the  $\text{C}_{4v}$   $\text{LiAl}_4^-$  to the highly fluxional [51]  $\text{C}_s$   $\text{Li}_2\text{Al}_4$  species aromaticity slightly decreases. Roy et al. reached the same conclusions based on NICS and MCI results [36]. The values of  $\text{MCI}_{\text{ovl}}$  and  $\delta_{\alpha}^{1,3}$  are indicative of larger reduction of the  $\sigma$ - than the  $\pi$ -aromatic character (in fact, there is an insignificant gain of  $\pi$ -aromaticity) while  $\text{MCI}_{\alpha}^{\text{orb}}$  values show a slight decrease in both  $\sigma$  and  $\pi$  contributions. This is due to the fact that the second  $\text{Li}^+$  interacts more strongly with the  $\sigma$ -orbitals, in particular with the tangential  $b_{2g}$  orbital. Taking the values of  $\text{Al}_4^{4-}$  in Table 1 as reference, we observed that when going from  $\text{Al}_4^{4-}$  to  $\text{C}_s$   $\text{Li}_2\text{Al}_4^{2-}$  there is an important decrease of the antiaromatic  $\pi$ -character of the  $\text{Al}_4$  unit, which is due to partial transfer of  $\pi$ -electrons from  $\text{Al}_4$  unit to the  $\text{Li}^+$  cations. Indeed the QTAIM electronic charge of the  $\text{Al}_4$  unit changes from  $-4.000$  au in  $\text{Al}_4^{4-}$  to  $-2.500$  au in  $\text{Li}_2\text{Al}_4^{2-}$ . The transfer of  $\sigma$ -electrons from  $\text{Al}_4$  unit to the  $\text{Li}^+$  cation, which is the farthest away from the center of the ring, produces a clear reduction in the  $\sigma$ -aromaticity as can be seen in the  $\text{MCI}_{\sigma}$  and  $\delta_{\sigma}^{1,3}$  values. MCI and  $\delta^{1,3}$  results of Table 3 indicate a reduction in aromaticity in the order  $\text{Li}_2\text{Al}_4^{2-} > \text{Li}_3\text{Al}_4^- \approx \text{Li}_4\text{Al}_4$ . The reduction in the MCI and  $\delta^{1,3}$  values when going from  $\text{C}_s$   $\text{Li}_2\text{Al}_4^{2-}$  to  $\text{C}_s$   $\text{Li}_3\text{Al}_4^-$  is more

important for the  $\pi$ - than for the  $\sigma$ -component. On the other hand, differences in electron delocalization and aromaticity between  $\text{C}_s$   $\text{Li}_3\text{Al}_4^-$  and  $\text{C}_{2v}$   $\text{Li}_4\text{Al}_4$  are minor. This result is in contradiction to the NICS(0) values of about  $-4.8$  ppm and  $-11.4$  ppm obtained for  $\text{C}_s$   $\text{Li}_3\text{Al}_4^-$  and  $\text{C}_{2v}$   $\text{Li}_4\text{Al}_4$  that point out an increase in aromaticity by adding a  $\text{Li}^+$  to  $\text{Li}_3\text{Al}_4^-$  [58]. Similarly, Roy et al. reported NICS(0) values of  $-5.7$ ,  $-5.4$  and  $-11.1$  ppm for  $\text{Al}_4^{4-}$ ,  $\text{Li}_3\text{Al}_4^-$ , and  $\text{Li}_4\text{Al}_4$  and MCI values of  $0.091$ ,  $0.073$ , and  $0.076$  for  $\text{Al}_4^{4-}$ ,  $\text{Li}_3\text{Al}_4^-$ , and  $\text{Li}_4\text{Al}_4$  [36].

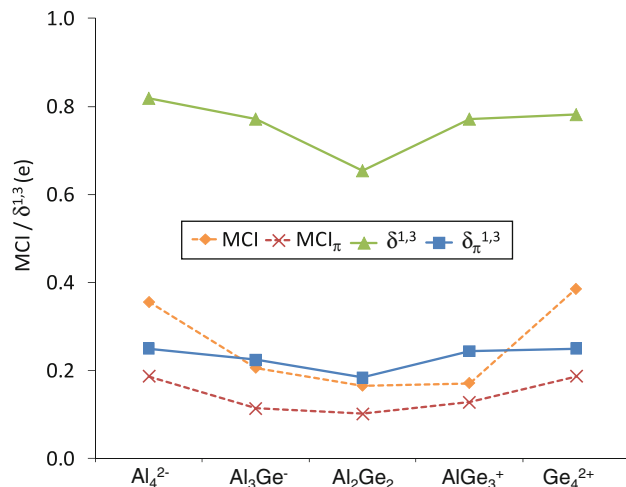
Table 4 collects the values of the MCI and  $\delta^{1,3}$  indices, while Fig. 3 depicts the trends for the MCI and  $\delta^{1,3}$  indices along the series  $\text{Al}_4^{2-}$  to  $\text{Ge}_4^{2+}$ . For this series, one can predict a steep decrease in aromaticity when going from  $\text{Al}_4^{2-}$  to, for instance,  $\text{GeAl}_3^-$  due to the reduction in symmetry and the substitution of one Al atom by a more electronegative Ge atom. A smooth reduction in aromaticity when going from  $\text{Al}_3\text{Ge}^-$  to  $\text{Al}_2\text{Ge}_2$  is also likely, although more questionable. And the same should occur from  $\text{Ge}_4^{2+}$  to  $\text{Al}_2\text{Ge}_2$ . Therefore, the expected order of aromaticity is  $\text{Al}_4^{2-} > \text{Al}_3\text{Ge}^- \geq \text{Al}_2\text{Ge}_2 \leq \text{AlGe}_3^+ < \text{Ge}_4^{2+}$ . Interestingly, both total MCI and  $\text{MCI}_{\pi}$  curves have a clear concave  $\cup$  shape providing the expected order of aromaticity. For symmetry reasons, the  $\text{MCI}_{\pi}$  values of  $\text{D}_{4h}$   $\text{Al}_4^{2-}$  and  $\text{Ge}_4^{2+}$  clusters with  $2\pi$ -electrons are exactly the same,  $0.187$  a.u.. It has to be mentioned that  $\text{MCI}_{\sigma}$  values (not shown in Fig. 3) fail by assigning a larger aromaticity to  $\text{Al}_2\text{Ge}_2$  than to  $\text{AlGe}_3^+$ . The correct shape is also provided by the  $\delta^{1,3}$  and  $\delta_{\pi}^{1,3}$  components ( $\delta_{\sigma}^{1,3}$  also gives the correct trend, see Table 4) of the total electronic delocalization. As found in organic molecules [41], for inorganic species the crossed term corresponding to the two farthest atoms in the ring (i.e.,  $\delta_{\alpha}^{1,3}$  in 4-MRs) is larger for the most aromatic member of a given series.

Since the study of the  $\text{Ta}_3\text{O}_3^-$ ,  $\text{Hf}_3$ ,  ${}^5\text{Ta}_3^-$ , and  ${}^3\text{Hf}_3$  species requires the inclusion of relativistic effects, we have employed pseudopotentials for the calculations. As a side effect, the use of pseudopotentials leads to spurious densities close to nuclei that result in the appearance of non-nuclear attractors in the QTAIM partition. This makes the calculation of the  $S_{ij}(A)$  terms cumbersome. For this reason, the overlap between MOs  $i$  and  $j$  within the molecular space assigned to atom  $A$  has been calculated for these molecules using the fuzzy atom partition. Table 5 compares the B3LYP/6-311+G(d) results of the MCI,  $\text{MCI}_{\alpha}$ ,  $\delta_{\alpha}^{1,3}$ , and  $\delta_{\pi}^{1,3}$  ( $\alpha = \sigma$  and  $\pi$ ) indices for  $\text{Al}_4^{2-}$  and  $\text{Al}_3\text{Ge}^-$  computed with the QTAIM and fuzzy atomic partitions of the molecular space. For  $\text{Al}_4^{2-}$ , the results obtained with the QTAIM and fuzzy partition differ by few hundredths of an electron. This is not surprising, since it is well known that for species involving only homonuclear bonds the different atomic partitions lead to very similar

**Table 4** MCI,  $MCI_{\alpha}$ ,  $\delta_{\alpha}^{1,3}$ , and  $\delta_{\pi}^{1,3}$  ( $\alpha = \sigma$  and  $\pi$ ) indices for the  $[Al_nGe_{4-n}]^{q\pm}$  ( $n = 0–4$ ) series at the B3LYP/6–311+G(d) level of theory

	$Al_4^{2-}$	$Al_3Ge^-$	$Al_2Ge_2$	$AlGe_3^+$	$Ge_4^{2+}$
					
Symmetry	D <sub>4h</sub>	C <sub>2v</sub>	C <sub>2v</sub>	C <sub>2v</sub>	D <sub>4h</sub>
MCI	0.356	0.206	0.165	0.171	0.386
$MCI_{\sigma}$	0.169	0.092	0.063	0.043	0.199
$MCI_{\pi}$	0.187	0.114	0.102	0.128	0.187
$\delta^{1,3}$	0.818	0.771	0.654	0.771	0.781
$\delta_{\sigma}^{1,3}$	0.568	0.546	0.469	0.527	0.531
$\delta_{\pi}^{1,3}$	0.250	0.224	0.184	0.244	0.250

All distances in Å and all delocalization values in atomic units

**Fig. 3** Variation of MCI,  $MCI_{\pi}$ ,  $\delta^{1,3}$ , and  $\delta_{\pi}^{1,3}$  (in electrons) along the series  $Al_4^{2-}$ ,  $Al_3Ge^-$ ,  $Al_2Ge_2$ ,  $AlGe_3^+$ , and  $Ge_4^{2+}$ 

atomic charges and multicenter ESI values [82, 95, 96]. The differences between QTAIM and fuzzy partitions are more noticeable in the case of the  $Al_3Ge^-$  species, but the qualitative trends are the same. Thus, the different QTAIM and fuzzy MCI and  $\delta_{\alpha}^{1,3}$  ( $\alpha = \sigma$  and  $\pi$ ) values indicate a reduction in aromaticity when going from  $Al_4^{2-}$  to  $Al_3Ge^-$ , although more evident in the case of the QTAIM partition. As found in a previous study [96], here we also observe that ESI values between non-bonded atoms ( $\delta_{\alpha}^{1,3}$  ( $\alpha = \sigma$  and  $\pi$ ) in our case) tend to be larger when using fuzzy atoms. Since for  $Ta_3O_3^-$ ,  $Ta_3^-$ , and  $Hf_3$  species, we analyze the aromaticity of the rings containing only homonuclear bonds (Ta-Ta or Hf-Hf), we expect that the fuzzy partition will produce results quite similar to those yielded by the QTAIM partition. In order to compare the aromaticity of transition-metal rings, the results of Tables 6

**Table 5** Comparison of the MCI,  $MCI_{\alpha}$ ,  $\delta^{1,3}$ , and  $\delta_{\alpha}^{1,3}$  ( $\alpha = \sigma$  and  $\pi$ ) indices for  $Al_4^{2-}$  and  $Al_3Ge^-$  computed with the QTAIM and fuzzy atomic partitions of the molecular space at the B3LYP/6–311+G(d) level of theory

	QTAIM $Al_4^{2-}$	FUZZY $Al_4^{2-}$	QTAIM $Al_3Ge^-$	FUZZY $Al_3Ge^-$
MCI	0.356	0.364	0.206	0.314
$MCI_{\sigma}$	0.169	0.177	0.092	0.147
$MCI_{\pi}$	0.187	0.187	0.114	0.167
$\delta^{1,3}$	0.817	0.874	0.771	0.799
$\delta_{\sigma}^{1,3}$	0.567	0.622	0.547	0.561
$\delta_{\pi}^{1,3}$	0.250	0.252	0.224	0.238

All values in atomic units

and 7 have been obtained using the fuzzy partition for all the 3-MR species.

In the next section, we will focus on the analysis of transition-metal rings with single, double, and triple aromatic character. Table 6 assembles the MCI values of the  $Cu_3^+$ ,  $Cu_3H_3$ ,  $Y_3^-$ , and  $La_3^-$  species. Yong et al. showed that the  $Cu_3^+$  unit is a single  $\sigma$ -aromatic system with only s-atomic orbitals (AO) involved in chemical bonding [59]. These observations were supported by MO analysis and NICS(0) and NICS(1) values of –28.22 and –12.31 ppm, respectively. Interestingly, the MCI values confirm the  $\sigma$ -aromaticity in  $Cu_3^+$  giving a large  $MCI_{\sigma}$  contribution (0.188 a.u.) while  $MCI_{\pi}$  is almost zero (0.001 a.u.). In 2003, Tsipis and Tsipis investigated the aromaticity of  $Cu_nH_n$  ( $n = 3–6$ ) cyclic species [60]. They concluded that these compounds are  $\sigma$ -aromatic due to the equivalence of Cu–Cu and Cu–H bonds. Moreover, Tsipis et al. performed NICS calculations, which also support the cyclic electron delocalization in these systems. However, in 2006, Lin et al. showed that  $Cu_4H_4$  did not sustain any strong magnetically

**Table 6** MCI,  $MCI_{\sigma}$ , and  $MCI_{\delta}$  indices for  $Cu_3^+$ ,  $Cu_3H_3$ ,  $Y_3^-$  and  $La_3^-$  at the B3LYP/X/Stuttgart+2f (X = Cu, Y, and La) level of theory computed with the fuzzy partition

	$Cu_3^+$	$Cu_3H_3$	$Y_3^-$	$La_3^-$
MCI	0.189	0.013	0.754	0.750
$MCI_{\sigma}$	0.188	0.013	0.458	0.454
$MCI_{\pi}$	0.001	0.000	0.296	0.296
$MCI_{\delta}$	0.000	0.000	0.000	0.000
Aromaticity	$\sigma$	—	$\sigma + \pi$	$\sigma + \pi$

All distances in Å and all delocalization values in atomic units

**Table 7** MCI,  $MCI_{\sigma}$ ,  $MCI_{\pi}$ , and  $MCI_{\delta}$  indices for the  $Ta_3$  unit in  $Ta_3O_3^-$ ,  $Hf_3$ ,  $^5Ta_3^-$ , and  $^3Hf_3$  at the B3LYP/X/Stuttgart+2f (X = Ta and Hf) level of theory computed with the fuzzy partition

	$Ta_3O_3^-$	$Hf_3$	$^5Ta_3^-$	$^3Hf_3$
MCI	0.584	1.037	0.776	0.653
$MCI_{\sigma}^{orb}$	0.111	0.445	0.362	0.453
$MCI_{\pi}^{orb}$	0.272	0.296	0.178	0.200
$MCI_{\delta}^{orb}$	0.201	0.295	0.235	0.000
$MCI^{ovl}$	0.624	1.038	0.878	0.653
$MCI_{\sigma}^{ovl}$	0.085	0.445	0.403	0.453
$MCI_{\pi}^{ovl}$	0.272	0.296	0.178	0.200
$MCI_{\delta}^{ovl}$	0.267	0.296	0.296	0.000
Error (%) <sup>a</sup>	6.90	0.16	13.5	0
Aromaticity	$\pi + \delta$	$\sigma + \pi + \delta$	$\sigma + \pi + \delta$	$\sigma + \pi$

<sup>a</sup> Calculated as  $\left| \frac{MCI - MCI^{ovl}}{MCI} \right| \times 100$ 

All distances in Å and all delocalization values in atomic units

induced ring current, and, then, this molecule should not be considered as aromatic [97]. In order to assess the aromaticity of  $Cu_nH_n$  species, we have analyzed the behavior of the electron delocalization in the  $Cu_3H_3$  molecule. As shown in Table 6, the MCI value of  $Cu_3H_3$  is practically zero in comparison with  $Cu_3^+$  unit. In addition, MCI values of 0.005, 0.001, and 0.000 a.u. have been found for  $Cu_4H_4$ ,  $Cu_5H_5$ , and  $Cu_6H_6$ , respectively. Consequently, according to these electron delocalization measures,  $Cu_nH_n$  ( $n = 3–6$ ) cyclic species cannot be considered as aromatic. In 2007, Chi and Liu found that  $D_{3h}$  structures for  $Sc_3^-$ ,  $Y_3^-$ , and  $La_3^-$  are d-orbital  $\sigma$ - and  $\pi$ -aromatic systems with large negative NICS values [61]. These species were the first reported transition-metal systems with double  $\sigma$ - and  $\pi$ -aromaticity. Their large  $MCI_{\sigma}$  and  $MCI_{\pi}$  values confirm the double aromatic character of  $Y_3^-$  and  $La_3^-$ .

Finally, we have analyzed the multifold aromaticity of a series of species with  $\delta$ -aromatic character. As said in the introduction,  $Ta_3O_3^-$  has double  $\pi$ - and  $\delta$ -aromaticity [10]. This is supported by the small  $MCI_{\sigma}$ , in comparison with  $Y_3^-$ ,  $La_3^-$ , and  $Hf_3$ , and the relatively large  $MCI_{\pi}$  and  $MCI_{\delta}$  values of Table 7. Interestingly, the large  $MCI_{\sigma}$  ( $\alpha = \sigma$ ,  $\pi$ , and  $\delta$ ) for  $Hf_3$  concurs with the  $\sigma$ -,  $\pi$ -, and  $\delta$ -aromaticity found in this inorganic cluster [11]. According to our results, the  $\pi$ - and  $\delta$ -aromatic character in  $Hf_3$  is similar and smaller than the  $\sigma$ -aromatic character. In addition, we have studied how the electronic delocalization measures describe the aromaticity in open-shell systems with multiple aromaticity. To this end, two  $D_{3h}$  species have been selected. First, quintet  $^5Ta_3^-$  which is the ground state for  $Ta_3^-$  anion [62] and, then,  $^3Hf_3$  which is the lowest triplet state for  $Hf_3$  [11]. In 2008, Wang et al. [62]

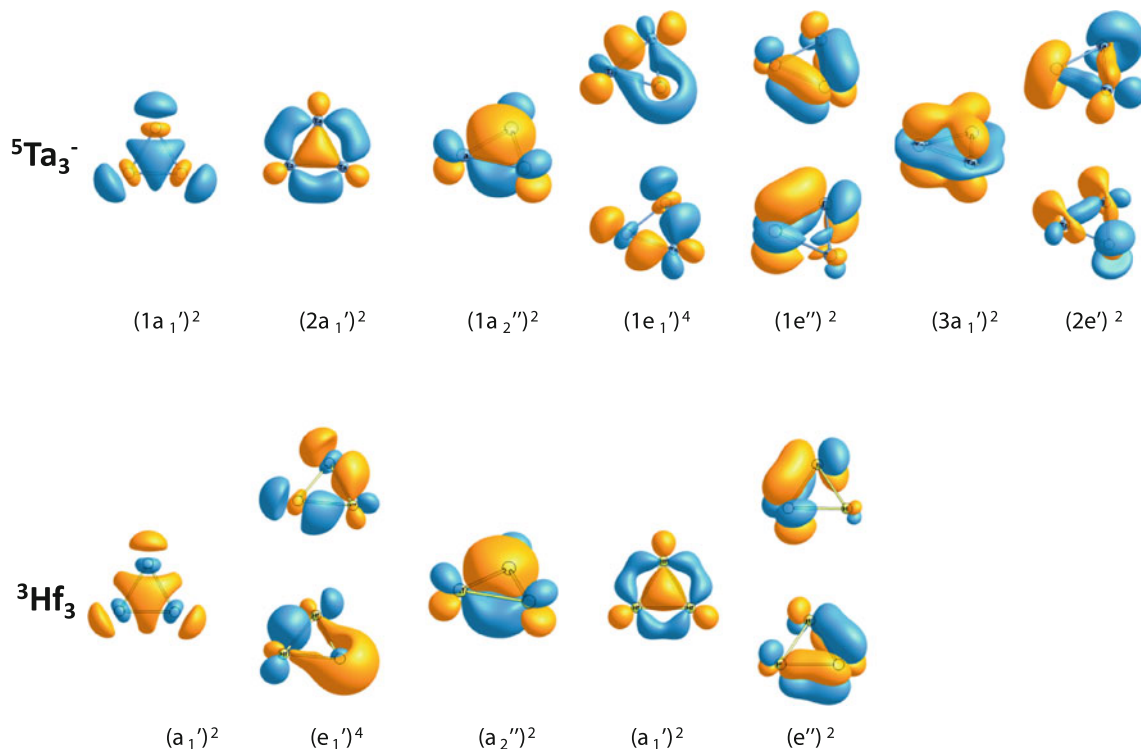


**Fig. 4** The low-lying occupied molecular orbitals of  ${}^5\text{Ta}_3^-$  and  ${}^3\text{Hf}_3$

studied the chemical bonding and aromaticity of lowest-lying states of  $\text{Ta}_3^-$  and they concluded by means of molecular orbital analysis that  ${}^5\text{Ta}_3^-$  possesses partial  $\sigma$ -, partial  $\pi$ -, and  $\delta$ -aromatic character. Our results confirm these trends, MCI values show a lower  $\sigma$ - and  $\pi$ -aromaticity than  $\sigma$ - $\pi$ -, and  $\delta$ -aromatic  $\text{Hf}_3$  or  $\sigma$ - and  $\pi$ -aromatic  $\text{Y}_3^-$  and  $\text{La}_3^-$  compounds while  $\delta$ -aromaticity is practically the same in  ${}^5\text{Ta}_3^-$  as in  $\text{Hf}_3$ . As shown in Table 7, the relative error for  ${}^5\text{Ta}_3^-$  is 13.5%, this is because the strong overlap between  $\sigma$  2e' and  $\delta$  3a<sub>1'</sub> orbitals (see Fig. 4), which prevents a better  $\sigma/\delta$  orbital separation. In comparison with  $\text{Ta}_3\text{O}_3^-$ ,  ${}^5\text{Ta}_3^-$  is more aromatic because the high  $\sigma$ -electron delocalization. Finally,  ${}^3\text{Hf}_3$  was presented by Averkiev et al. as the lowest triplet state of  $\text{Hf}_3$  with  $\sigma$ - and  $\pi$ -aromaticity [11]. MCI values also reproduce these observations. In comparison with  ${}^1\text{Hf}_3$ , MCI <sub>$\sigma$</sub>  contribution to the aromaticity of  ${}^3\text{Hf}_3$  is more or less the same than the lowest lying singlet state while the  $\pi$ -contribution is reduced 0.1 a.u. due to the single occupation of e'' orbitals in  ${}^3\text{Hf}_3$  (see Fig. 4). Consequently,  ${}^1\text{Hf}_3$  is more aromatic than  ${}^3\text{Hf}_3$  because the first presents  $\delta$ -aromaticity and its  $\pi$ -aromaticity is somewhat larger. It is worth to mention that  ${}^5\text{Ta}_3^-$  and  ${}^3\text{Hf}_3$  have four  $\pi$ -electrons that follow the Baird's rule stating that the lowest lying triplet states with 4n  $\pi$ -electrons are  $\pi$ -aromatic [98].

In summary, our results show that the  $\sigma$ -,  $\pi$ -, and  $\delta$ -components of the multicenter indices are excellent

indicators of  $\sigma$ -,  $\pi$ -, and  $\delta$ -aromaticity in inorganic clusters. We consider that these indices can be very helpful in the non-trivial task of assigning the aromatic character of all-metal and semimetal clusters. The  $\sigma$ -,  $\pi$ -, and  $\delta$ -crossed contributions to the total electronic delocalization corresponding to the two farthest atoms in the ring (i.e.,  $\delta_x^{1,3}$  in 4-MRs) are also good descriptors of aromaticity.

#### 4 Conclusions

The quantitative evaluation of aromaticity in inorganic clusters is cumbersome due to the lack of aromatic inorganic systems that can be used as a reference. Basically, the aromaticity of these species can only be assessed by the use of the simple Hückel's 4n+2 rule and the calculation of the NICS and MCI descriptors. Simple total electronic count is a vague criterion that depends on the number of valence orbitals that one considers delocalized and may lead sometimes to incorrect results [8, 49, 99, 100]. In addition, electron counting does not provide a quantitative value, so comparisons of aromaticity from different compounds are not possible. Moreover, in previous works [38, 101], we have reported that the behavior of MCI is superior to that of the NICS magnetic-based index. In this work, we show that MCI of planar (or pseudo-planar) species can be separated into the  $\sigma$ -,  $\pi$ -, and  $\delta$ -components.

These  $MCI_\alpha$  ( $\alpha = \sigma, \pi$ , and  $\delta$ ) indices provide quantitative valuable information about the type of aromaticity that a certain aromatic inorganic cluster has. The  $MCI_\alpha$  results reported for all systems studied in the present work were in line with previous classifications of the species according to their aromatic character. The results obtained are invariant with respect to unitary transformation of the molecular orbitals and the errors associated with the partition are measurable and are, in general, minor. Therefore, the use of MCI and its components is recommended in the analysis of aromaticity of all-metal and semimetal clusters. Finally, our results show that the crossed term corresponding to the two farthest atoms in the ring (i.e.,  $\delta_\pi^{1,3}$  in 4-MRs) decreases also in aromatic inorganic species when two electrons are added or removed and that this crossed term is higher for the most aromatic molecule in a series of same-membered rings. Consequently, this crossed term, which is less computationally demanding than MCI, is also a good descriptor of aromaticity in all-metal and semimetal clusters.

**Acknowledgments** Financial help has been furnished by the Spanish MICINN project no. CTQ2008-03077/BQU and by the Catalan DIUE through project no. 2009SGR637. F.F. and J.P. thank the MICINN for the doctoral fellowship no. AP2005-2997 and the Ramón y Cajal contract, respectively. E.M. acknowledges financial support from the Lundbeck Foundation Center and from Marie Curie IntraEuropean Fellowship, Seventh Framework Programme (FP7/2007-2013), under grant agreement no. PIEF-GA-2008-221734 and from the Polish Ministry of Science and Higher Education (Project no. N N204 215634). Support for the research of M.S. was received through the ICREA Academia 2009 prize for excellence in research funded by the DIUE of the Generalitat de Catalunya. We thank the Centre de Supercomputació de Catalunya (CESCA) for partial funding of computer time.

## References

- Faraday M (1825) Philos Trans R Soc London 115:440
- Poater J, Duran M, Solà M, Silvi B (2005) Chem Rev 105:3911
- Merino G, Vela A, Heine T (2005) Chem Rev 105:3812
- Chen Z, Wannere CS, Corminboeuf C, Puchta R, Schleyer PvR (2005) Chem Rev 105:3842
- Li X, Kuznetsov AE, Zhang H-F, Boldyrev A, Wang L-S (2001) Science 291:859
- Boldyrev AI, Wang L-S (2005) Chem Rev 105:3716
- Tsipis CA (2005) Coord Chem Rev 249:2740
- Zubarev DY, Averkiev BB, Zhai H-J, Wang L-S, Boldyrev AI (2008) Phys Chem Chem Phys 10:257
- Huang X, Zhai H-J, Kiran B, Wang L-S (2005) Angew Chem Int Ed 44:7251
- Zhai H-J, Averkiev BB, Zubarev DY, Wang L-S, Boldyrev AI (2007) Angew Chem Int Ed 46:4277
- Averkiev BB, Boldyrev AI (2007) J Phys Chem A 111:12864
- Tsipis AC, Kefalidis CE, Tsipis CA (2008) J Am Chem Soc 130:9144
- Zhan C-G, Zheng F, Dixon DA (2002) J Am Chem Soc 124:14795
- Zhai H-J, Kuznetsov AE, Boldyrev A, Wang L-S (2004) ChemPhysChem 5:1885
- Liu Z-Z, Tian W-Q, Feng J-K, Zhang G, Li W-Q (2005) J Phys Chem A 109:5645
- Chi XX, Chen XJ, Yuan ZS (2005) J Mol Struct (Theochem) 732:149
- Kruszewski J, Krygowski TM (1972) Tetrahedron Lett 13:3839
- Krygowski TM (1993) J Chem Inf Comp Sci 33:70
- Matito E, Duran M, Solà M (2005) J Chem Phys 122:014109
- Bultinck P, Ponec R, Van Damme S (2005) J Phys Org Chem 18:706
- Matta CF (2003) J Comput Chem 24:453
- Matta CF, Hernández-Trujillo J (2003) J Phys Chem A 107:7496
- Cyrański MK (2005) Chem Rev 105:3773
- Boldyrev AI, Kuznetsov AE (2002) Inorg Chem 41:532
- Matito E, Poater J, Duran M, Solà M (2005) J Mol Struct (Theochem) 727:165
- Hückel E (1931) Z Physik 70:104
- Hückel E (1931) Z Physik 72:310
- Hückel E (1932) Z Physik 76:628
- Hückel E (1937) Z Elektrochemie 43:752
- Schleyer PvR, Maerker C, Dransfeld A, Jiao H, van Eikema Hommes NJR (1996) J Am Chem Soc 118:6317
- Giambiagi M, de Giambiagi MS, dos Santos CD, de Figueiredo AP (2000) Phys Chem Chem Phys 2:3381
- Bultinck P, Rafat M, Ponec R, van Gheeluwe B, Carbó-Dorca R, Popelier P (2006) J Phys Chem A 110:7642
- Mandado M, González-Moa MJ, Mosquera RA (2007) J Comput Chem 28:127
- Cioslowski J, Matito E, Solà M (2007) J Phys Chem A 111:6521
- Mandado M, Krishtal A, Van Alsenoy C, Bultinck P, Hermida-Ramón JM (2007) J Phys Chem A 111:11885
- Roy DR, Bultinck P, Subramanian V, Chatteraj PK (2008) J Mol Struct Theochem 854:35
- Jiménez-Halla JOC, Matito E, Blancafort L, Robles J, Solà M (2009) J Comput Chem 30:2764
- Feixas F, Jiménez-Halla JOC, Matito E, Poater J, Solà M (2010) J Chem Theory Comput 6:1118
- Solà M, Feixas F, Jiménez-Halla JOC, Matito E, Poater J (2010) Symmetry 2:1156
- Feixas F, Matito E, Solà M, Poater J (2008) J Phys Chem A 112:13231
- Feixas F, Matito E, Solà M, Poater J (2010) Phys Chem Chem Phys 12:7126
- Jusélius J, Straka M, Sundholm D (2001) J Phys Chem A 105:9939
- Fowler PW, Havenith RWA, Steiner E (2001) Chem Phys Lett 342:85
- Fowler PW, Havenith RWA, Steiner E (2002) Chem Phys Lett 359:530
- Santos JC, Tiznado W, Contreras R, Fuentealba P (2004) J Chem Phys 120:1670
- Chatteraj PK, Roy DR, Elango M, Subramanian V (2005) J Phys Chem A 109:9590
- Lin YC, Jusélius J, Sundholm D, Gauss J (2005) J Chem Phys 122:214308
- Havenith RWA, van Lenthe JH (2004) Chem Phys Lett 385:198
- Havenith RWA, Fowler PW, Steiner E, Shetty S, Kanhere D, Pal S (2004) Phys Chem Chem Phys 6:285
- Datta A, Patti SK (2005) J Chem Theory Comput 1:824
- Islas R, Heine T, Merino G (2007) J Chem Theory Comput 3:775
- Mang C, Liu C, Wu K (2010) Int J Quantum Chem 110:1127
- Mang C, Liu C, Zhou J, Li Z, Wu K (2010) Chem Phys Lett 438:20
- Li X, Zhang H-F, Wang L-S, Kuznetsov AE, Cannon NA, Boldyrev AI (2001) Angew Chem Int Ed 40:1867

55. Seal P (2009) *J Mol Struct Theochem* 893:31
56. Nigam S, Majumder C, Kulshreshtha SK (2005) *J Mol Struct Theochem* 755:187
57. Kuznetsov AE, Birch KA, Boldyrev AI, Zhai H-J, Wang L-S (2003) *Science* 300:622
58. Chen Z, Corminboeuf C, Heine T, Bohmann J, Schleyer PvR (2003) *J Am Chem Soc* 125:13930
59. Yong L, Wu SD, Chi XX (2007) *Int J Quantum Chem* 107:722
60. Tsipis AC, Tsipis CA (2003) *J Am Chem Soc* 125:1136
61. Chi XX, Liu Y (2007) *Int J Quantum Chem* 107:1886
62. Wang B, Zhai H-J, Huang X, Wang L-S (2008) *J Phys Chem A* 112:10962
63. Frisch MJ, Trucks GW, Schlegel HB, Scuseria GE, Robb MA, Cheeseman JR, Montgomery JA Jr, Vreven T, Kudin KN, Burant JC, Millam JM, Iyengar SS, Tomasi J, Barone V, Mennucci B, Cossi M, Scalmani G, Rega N, Petersson GA, Nakatsuji H, Hada M, Ehara M, Toyota K, Fukuda R, Hasegawa J, Ishida M, Nakajima T, Honda Y, Kitao O, Nakai H, Klene M, Li X, Knox JE, Hratchian HP, Cross JB, Bakken V, Adamo C, Jaramillo J, Gomperts R, Stratmann RE, Yazyev O, Austin AJ, Cammi R, Pomelli C, Ochterski JW, Ayala PY, Morokuma K, Voth GA, Salvador P, Dannenberg JJ, Zakrzewski G, Dapprich S, Daniels AD, Strain MC, Farkas O, Malick DK, Rabuck AD, Raghavachari K, Foresman JB, Ortiz JV, Cui Q, Baboul AG, Clifford S, Cioslowski J, Stefanov BB, Liu G, Liashenko A, Piskorz P, Komaromi I, Martin RL, Fox DJ, Keith T, Al-Laham MA, Peng CY, Nanayakkara A, Challacombe M, Gill PMW, Johnson B, Chen W, Wong MW, Gonzalez C, Pople JA (2003) Gaussian 03. Gaussian, Inc, Pittsburgh, PA
64. Stephens PJ, Devlin FJ, Chabalowski CF, Frisch MJ (1994) *J Phys Chem* 98:11623
65. Becke AD (1993) *J Chem Phys* 98:5648
66. Lee C, Yang W, Parr RG (1988) *Phys Rev B* 37:785
67. Frisch MJ, Pople JA, Binkley JS (1984) *J Chem Phys* 80:3265
68. Krishnan R, Binkley JS, Seeger R, Pople JA (1980) *J Chem Phys* 72:650
69. Andrae D, Haeussermann U, Dolg M, Stoll H, Preuss H (1990) *Theor Chim Acta* 77:123
70. Küchle W, Dolg M, Stoll H, Preuss H (1994) *J Chem Phys* 100:7535
71. Dunning TH Jr (1989) *J Chem Phys* 90:1007
72. Kendall RA, Dunning TH Jr, Harrison RJ (1992) *J Chem Phys* 96:6796
73. Lambrecht DS, Fleig T, Sommerfeld T (2008) *J Phys Chem A* 112:2855
74. Zubarev DY, Boldyrev AI (2008) *J Phys Chem A* 112:7984
75. Lambrecht DS, Fleig T, Sommerfeld T (2008) *J Phys Chem A* 112:7986
76. Fradera X, Austen MA, Bader RFW (1999) *J Phys Chem A* 103:304
77. Fradera X, Poater J, Simon S, Duran M, Solà M (2002) *Theor Chem Acc* 108:214
78. Matito E, Solà M, Salvador P, Duran M (2007) *Faraday Discuss* 135:325
79. Ruedenberg K (1962) *Rev Mod Phys* 34:326
80. Mandado M, González-Moa MJ, Mosquera RA (2007) *ChemPhysChem* 8:696
81. Güell M, Matito E, Luis JM, Poater J, Solà M (2006) *J Phys Chem A* 110:11569
82. Matito E, Poater J, Solà M, Duran M, Salvador P (2005) *J Phys Chem A* 109:9904
83. Ponec R, Cooper D (2005) *J Mol Struct Theochem* 727:133
84. Bader RFW (1985) *Acc Chem Res* 18:9
85. Bader RFW (1990) Atoms in Molecules: A Quantum Theory. Clarendon, Oxford
86. Bader RFW (1991) *Chem Rev* 91:893
87. Biegler-König FW, Bader RFW, Tang T-H (1982) *J Comput Chem* 3:317
88. Matito E (2006) ESI-3D: electron sharing indexes program for 3D molecular space partitioning, <http://iqc.udg.es/~eduard/ESI>. Girona, Institute of Computational Chemistry
89. Mayer I, Salvador P (2004) *Chem Phys Lett* 383:368
90. Salvador P, Mayer I (2004) *J Chem Phys* 120:5046
91. Mayer I, Salvador P (2003) Program FUZZY. Girona, Available from <http://occam.chemres.hu/programs>
92. Suresh CH, Koga N (2001) *J Phys Chem A* 105:5940
93. Becke AD, Edgecombe KE (1990) *J Chem Phys* 92:5397
94. Corminboeuf C, Heine T, Weber J (2003) *Phys Chem Chem Phys* 5:246
95. Matito E, Salvador P, Duran M, Solà M (2006) *J Phys Chem A* 110:5108
96. Heyndrickx W, Salvador P, Bultinck P, Solà M, Matito E (2010) *J Comput Chem*. doi:[10.1002/jcc.21621](https://doi.org/10.1002/jcc.21621)
97. Lin YC, Sundholm D, Juselius J, Cui LF, Li X, Zhai HJ, Wang LS (2006) *J Phys Chem A* 110:4244
98. Baird NC (1972) *J Am Chem Soc* 94:4941
99. Jung Y, Heine T, Schleyer PvR, Head-Gordon M (2004) *J Am Chem Soc* 126:3132
100. Aihara J, Kanno H, Ishida T (2005) *J Am Chem Soc* 127:13324
101. Feixas F, Matito E, Poater J, Solà M (2008) *J Comput Chem* 29:1543